Electrochemical and Mechanical characterization of Ni/SiC composite coatings electrodeposited on steel

Ghelani. L[1], Boulahrouz. S[1], Naoun. M[2] and Aissani[1]. L

[1] *Mechanical Engineering Department, Faculty of Technology and Science, University of Khenchela 40000, Algeria.*
[2] *Mechanical Engineering Department, Faculty of technology, University of Batna 2, 05000, Batna, Algerie.*
ghilanilaala@yahoo.fr,
boulahrouz_salim@yahoo.fr,
mnaoun@yahoo.fr,
lindaaissani2004@yahoo.fr.

***Abstract* — In this study, the structure (Ni/SiC) composite and pure nickel coatings were prepared by electroplating deposition on steel in a Watts bath of electroplating chloride, consisting of an electrolytic nickel matrix (binder) with and without adding silicon carbide micro particles (SiC) (mean diameter 0.8 μm) which a high hardness and a good chemical stability.**

The coating analysis is performed by atomic force microscopy (AFM), and scanning electron microscopy (SEM). The characterizations of the deposited layers are carried out in 3.5% NaCl solution. The weight loss and the polarization results highlighted a silicon carbide concentration which can be included in the overall expression of a good composite coating. Moreover, the incorporation of the micro particles had a significant impact on the micro hardness of the composite deposits (Ni / SiC).

***Keywords* — electrodeposition, co-deposition, SiC, weight loss, polarization.**

I. INTRODUCTION

Various techniques are applied for the realization of composite coatings such as PVD, CVD, ion implantation etc. [1–3]. The composite coatings can also be obtained by deposition. This method also includes techniques for making deposits of material on the surface of the base materials from a bath loaded with suspended particles. Among these methods, electrodeposition is one of the efficient and cost-effective methods that can utilize a wide range of substrate sizes and reinforcements [4–7]. Most researchers use nickel as a matrix and ceramics as reinforcement [8–9].
The improvement of the process begins with the reliability of the methods of preparation of the surfaces allowing a good adhesion on the metal supports.

Electrodeposition is considered one of the reliable techniques for producing composite deposits. Recently a number of literature reports that (SiC) can be co-deposited to form composite coatings [10–14]. Silicon carbide (SiC) is a ceramic compound that can be used in various scientific fields. The presence of these particles in the coating layers modifies mechanical properties resistance to corrosion, wear and micro hardness. SiC is much more recommended for industrial applications [15–18]. These properties are mainly due to the strong covalent bond between silicon and carbon and for tetrahedral coordination. The first applications of coatings (Ni SiC) appeared in the industry [19 –20].

The development of these composite coatings leads to much better properties than materials made from simple coatings. This is probably due to the possibilities of combining the characteristics of the base materials and the composite coatings.

In this study we carried out various tests to determine the best SiC concentration in a nickel matrix. It concerns the realization of composite coatings (Ni–SiC) on XC45 steel substrate tested in 3.5% NaCl solution. The results obtained show an improvement of the characteristics in particular behavior toward corrosion.

II. MATERIALS AND METHODS

A. Materials

The steel retained in this study is a grade XC45 steel, the chemical composition is determined by X-ray diffraction (Table I).

TABLE I. STEEL CHEMICAL COMPOSITION.

Chemical element	C	Si	Mn	P	S	Cr	Cu	Ni	Fe
Composition (%)	0.46	0.27	0.6	0.030	0.035	0.25	0.25	0.30	Bal

Two types of samples were prepared:

1st Type

The first type used for immersion and potentiostatic tests. Cylindrical pieces 6 mm diameter and 60 mm length (Fig. 1). They were cut from cylindrical rebar.

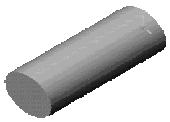

Fig.1. Cylindrical specimen.

2nd Type

These specimens were used for micrographic examinations. They are rectangular pieces, 1.8 x 20 x 25 mm. They were cut from XC45 steel sheet, surfaced on a horizontal milling machine and cut (Fig. 2).

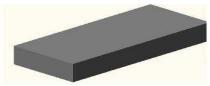

Fig.2. Rectangular specimen.

B. Samples preparation

The samples were prepared according to the following schematic steps (Fig. 3). Between two successive operations the piece was rinsed with distilled water, removing all contaminants from the surface [21].

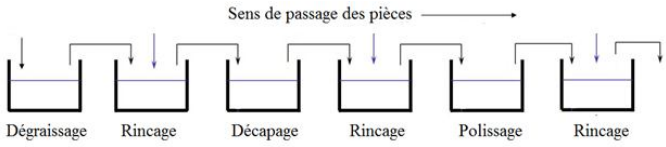

Fig.3. Surface preparation main steps

1. Degreasing

Degreasing was carried out as follows [22] :

A. Cold chemical degreasing consists of an ultrasonic cleaning of the specimens in acetone for 10 min.

B. The hot chemical degreasing is carried out by immersion of the sample in a bath whose composition and operating conditions are given below :

- Sodium hydroxide (NaOH) : 15 (g L^{-1}) ;
- Carbonates of soda (Na_2CO_3) : 30 (g L^{-1}) ;
- Tri-sodium phosphate (Na_3PO_4) : 60 (g L^{-1}) ;
- Sodium silicates (Na_2SiO_3) : 35 (g L^{-1});
- Temperature : 80 °C;
- Treatment time : 35 s

After degreasing, the samples were rinsed with distilled water.

C. Chemical deburring

This step follows degreasing. It was carried out in two different solutions. The first solution is basic and allows the elimination of any oxide. Its composition and operating conditions are summarized as follows [23]:

- Caustic soda : 15 (g L^{-1});
- Temperature : 65 °C;
- Treatment time : 3 min.

The second solution is sulfochromic which prevents the formation of the oxide layer which spontaneously covers the surface in contact with air. Its composition and its operating conditions are also given below.

- Sulfuric acid (d = 1,83) : 180 (ml L^{-1}) ;
- Chromic acid : 60 (g L^{-1}) ;
- Temperature : 55 °C;
- Treatment time : 10 min.

After each step the samples are rinsed with distilled water.

D. Mechanical polishing

Microscopic observation requires mirror polishing of the deposit surface. The samples are polished with SiC paper from 400 to 2400 with lubrication until mirror state of the surface is obtained [24].

E. Electrolytic polishing

It is based on the principle of anodic dissolution. The piece to be treated was placed in an electrolyte with the following composition and operating conditions [25]:

- H_3PO_4 : 60 (%);
- H_2SO_4 : 60 (%);
- CrO_3 : 9 (%);
- Temperature : 80 °C;
- Current density : 3 $A.dm^{-2;}$
- Cathodes : Pb – Sb.

C. Bath preparation [26 –28].

The bath composition is given in Table II.

TABLE II. BATH OF WATTS' CHLORIDE COMPOSITION

Bath composition	$NiCl_2+6H_2O$	NH_4Cl	NaCl	H_3BO_3	SiC
Concentration (g/l)	11.885	12.303	4.091	6.183	5 – 30

D.Deposits preparation

The composite deposits were made by adding silicon carbide (SiC) in the electrolyte with concentrations varying from 0g/l to 30g/l in steps of 5g/l. The electrodeposition parameters are presented in Table III.

TABLE III. ELECTRODEPOSITION PARAMETERS.

Operating conditions	
Electrical intensity	60 mA
Time of deposit	60 s
Temperature	50 °C
Agitation	Magnetic (200 $tr.mn^{-1}$)
Anodes	Soluble nickel plates
Cathodes	Substract
pH	4.5

E. Experimental device

The nickel-plating process device is shown in Fig. 4.

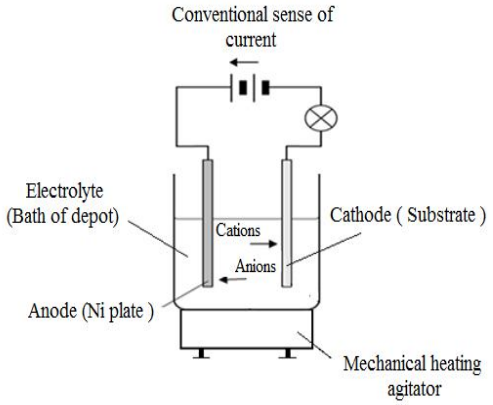

Fig. 4. Experimental device for electrolytic nickel plating.

F. Co-déposition

The principle of electrolytic co-deposition rests on the possibility of incorporating into electrolytic deposits (Or catalysts) solid particles held in suspension in the electrolytic bath. The degree of incorporation is function of the current intensity, the particles concentration in the bath and the mass transport along the cathode. Electrolytic co-deposition in our work is the incorporation of solid silicon carbide particles (SiC) in the catholic deposit. During the electrolysis these particles are incorporated in the metal deposit obtained at the cathode following the reduction of the metal ions present in the electrolysis bath. The composite deposit mechanism is schematized in the Figure 5.

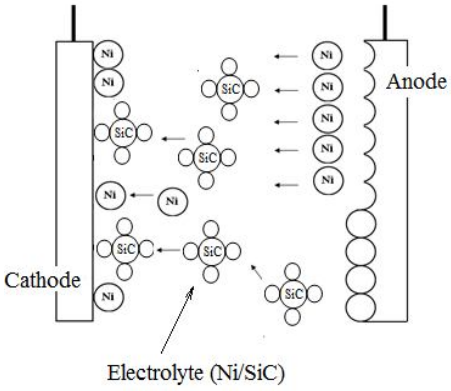

Fig. 5. Co-deposition process.

G. Degazage

The degassing heat treatment is carried out at 180 °C for one hour in order to eliminate the brittleness of the coated parts due to the presence of hydrogen trapped in the defects during the various treatments of the sample (mechanical or thermal).

H. Ni / SiC coatings characterization

The behavior of composite coatings (Ni/SiC) for different concentrations of SiC on steel substrates toward corrosion in 3.5% NaCl was determined by the following methods:

1. Weight loss

The aim of this method is to measure the mass lost of each specimen after a 15 day immersion in a corrosive medium (3.5% NaCl) with the presence of different concentrations of SiC. The specimens are weighed on an analytical scale of the type OHAUS AR 125CN. Following immersion, the specimens were reweighted after surface cleaning which removes any corrosion deposition from the surface. They were then, rinsed with distilled water and drying. The corrosion rate was calculated according to the formula below [29].

$$R_{corr} = \frac{\Delta m.10}{\rho.S}.\frac{365}{t} \quad (1)$$

$$\Delta m = m_1 - m_2$$

With:

- $R_{corr:}$ Corrosion rate (mm.an^{-1});
- m_1 : Initial mass of the specimen before immersion (g);
- m_2 : Final mass of the specimen after immersion (g);
- S : Surface of the specimen (cm^2);
- ρ : Density of nickel (8,902 g.cm^{-3});
- t : Immersion time (days).

2. Electrochemical polarization

The polarization tests were carried out in distilled water electrolyte containing 3.5% NaCl, with a Potentiostat Voltalab PGP 201 and a three-electrode cell; the working electrode, a platinum counter electrode and a saturated calomel reference electrode [30 − 31]. The scanning speed was 10 mV. Min^{-1}.

3. Micro hardness tests (hardness Vickers HV)

The Vickers hardness measurements (HV) were carried out on samples cut into the shape of a prism. These tests used an analytical microduometer type AFFRI 1-21056 INDULODONA. Due to the relatively low thickness of the deposited layers we chose a load F = 1 kN and 15 seconds penetration time. The values of the micro hardness were determined by the following formula [32−33]:

$$H_v = \frac{1,854 \quad F}{d^2} \quad (2)$$

- H_V: Vickers durete (kN.mm^{-2});
- F : Test load (kN);
- d : Average of the diagonals of the impression (d_1 and d_2) (mm) ;

With:

$$d = \frac{d_1 + d_2}{2}$$

4. Analysis by Atomic Force Microscopy (AFM)

The microscope used is AFM.100.APE research Nanotechnology multimode type. We applied the contact mode for good lateral imaging resolution. This allowed us to show the very fine variations of the morphology.

5. Scanning electron microscope (SEM) analysis

The surface morphologies of the deposits were characterized using a JEOL JSM 5900 LV scanning electron microscope, coupled to the Oxford Energy Incompatible Spectrometer (INCA x - act) spectrometer.

III. RESULTS AND INTERPRETATIONS

A. Influence of SiC concentration on corrosion behavior of coated XC45 steel .

1. Weight loss testing

The results are presented in Table IV.

TABLE IV. CORROSION RATE OF THE SPECIMENS AS A FUNCTION OF DIFFERENT SIC CONCENTRATIONS.

SiC Concentration (g/l)	m_1 (g)	m_2 (g)	Δm (g)	S (cm^2)	Corrosion rate (mm.an^{-1})
00	3.4900	3.4739	0.0161	11.8692	0.03709
05	3.4900	3.4820	0.0080	11.8692	0.01843
10	3.5569	3.5541	0.0028	11.8692	0.00645
15	3.5800	3.5790	0.0010	11.8692	0.00230
20	3.5523	3.5486	0.0037	11.8692	0.00852
25	3.5451	3.5368	0.0083	11.8692	0.01912
30	3.5528	3.5399	0.0129	11.8692	0.02972

From Table 4, we note that the corrosion rate decreases with the increase of SiC concentration up to 15 g/l. This decrease is due to the presence of the SiC particles (known for its improved physical and chemical properties [34–37]) in the coating layers leading to the improvement of the corrosion resistance. These properties are mainly due to the very solid covalent bond between silicon and carbon as well as for tetrahedral coordination. The homogeneity of the distribution of constituents (SiC) as determined by atomic force microscopy (Fig.13) and the possibilities of combining the characteristics of base metals and their coatings.

Following the observation of the samples after immersion in the electrolyte (pH2.5) and according to the nature of the nickel coating on the steel (cathodic coating), we note that for SiC concentrations above 20 g/l, the surface corrosion is pitting corrosion (the number of pits increases with the increase in SiC content). This is probably due to the creation of micropiles on the surface of the substrate resulting from the heterogeneity in the deposit on one hand and the presence of pure Ni in the coating shown in the DRX analysis (Fig. 9(a)) on the other hand the formation of galvanic cells.

2. Polarization curves

The current/voltage curves are obtained by performing a potential sweep from −850 mV/SCE up to +850 mV/SCE. Corrosion currents were obtained for different silicon carbide (SiC) concentrations from Tafel. The estimated corrosion rates are given in Table 5 and Fig. 6 and 7.

TABLE V. ESTIMATED CORROSION RATES OF NICKELETED SPECIMENS IN 3.5% NACL (PH4.5) IN THE PRESENCE OF DIFFERENT SIC CONCENTRATIONS .

SiC Concentration (g/l)	E_{corr} (mV/SCE)	$I_{corr.}$ (mA.cm^{-2})	Corrosion rates (mm.an^{-1})
00	- 475.7	0.0078	0.091
05	- 461.5	0.0057	0.066
10	- 504.4	0.0025	0.030
15	- 438.9	0.0023	0.027
20	- 517.7	0.0031	0.037
25	- 493.1	0.0047	0.055
30	- 473.3	0.0059	0.069

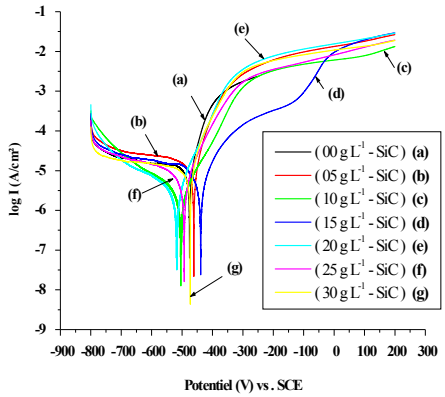

Fig. 6. Polarization curves of composite Ni/SiC deposits in 3.5% NaCl solution for different SiC concentrations (pH 4.5).

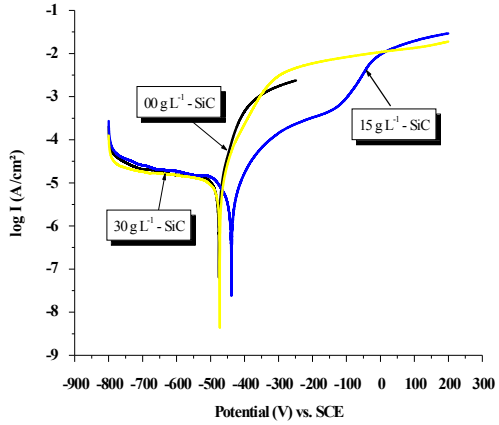

Fig. 7. Polarization curves of composite deposits (Ni / SiC) in a 3.5% NaCl solution (pH 4.5).

According to the results obtained we note a gradual decrease in the corrosion rate estimated as a function of the increase in the concentration of silicon carbide added up to the concentration of 15 g/l. And beyond this latter the corrosion rate increases with the increase of SiC concentrations. The corrosion rate variations have the same appearance as those obtained by the weight loss technique.

3. *Micro hardness measurement*

Each measurement was repeated 5 times and the average value was reported in Table VI. These results are in close agreement with the theory that predicts the increase in hardness with the increase in SiC content (Table VI).

TABLE VI . VICKERS MICRO HARDNESS FOR DIFFERENT COMPOSITE DEPOSITS NI/SIC.

SiC Concentration (g/l)	d_1 (µm)	d_2 (µm)	D (µm)	Vickers micro hardness
0	89.3	85.7	87.5	242.16
5	86.4	82.8	84.6	259.04
10	85.4	82.5	83.95	263.07
15	88.5	75.3	81.9	276.40
20	81.2	81.8	81.5	279.12
25	80.0	80.2	80.1	288.96
30	78.5	80.9	79.7	291.87

4. *Atomic Force Microscopy (AFM) observations*

Using the Atomic Force Microscopic analysis (AFM) to analyze the composite deposits (Ni SiC), we observe a significant evolution of the deposit morphology as a function of the introduction of SiC. The deposits without SiC particles exhibit a very smooth morphology with rare nodules (Fig. 9a). As the silicon carbide content increases the deposits become rough and the number of nodules increases. We also observe a microstructural refinement of the deposits as a function of the increase in the content of silicon carbide. The images clearly show SiC particles with conical heads (shiny points) embedded in the nickel matrix (Fig. 9 (b) to 9 (g)).

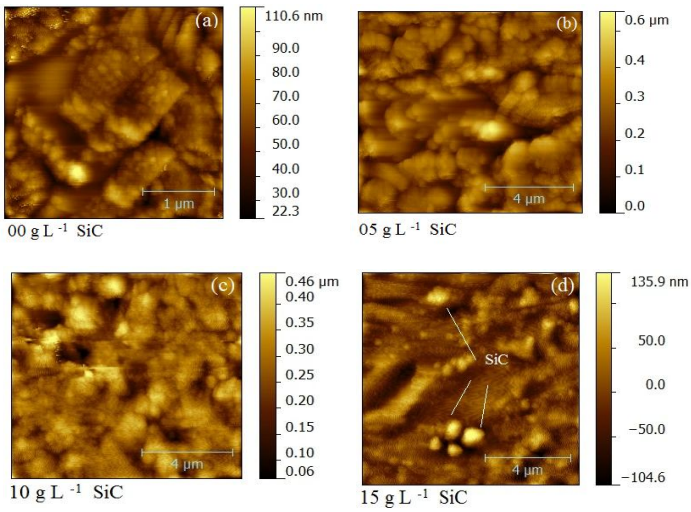

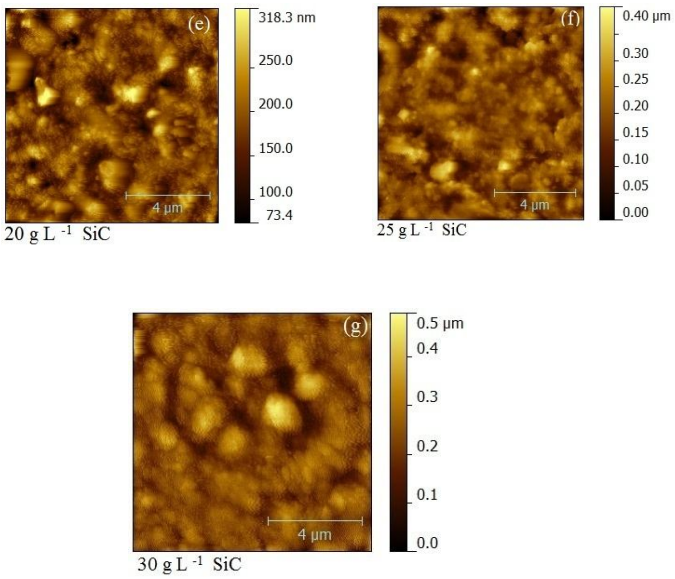

Fig. 9. Surface states of composite N/SiC coatings for different concentrations of SiC observed by AFM (x 400).

F. Scanning electron microscope (SEM) Observation.

The results of the SEM analysis of the composites (Ni / SiC) are presented in the figures below.

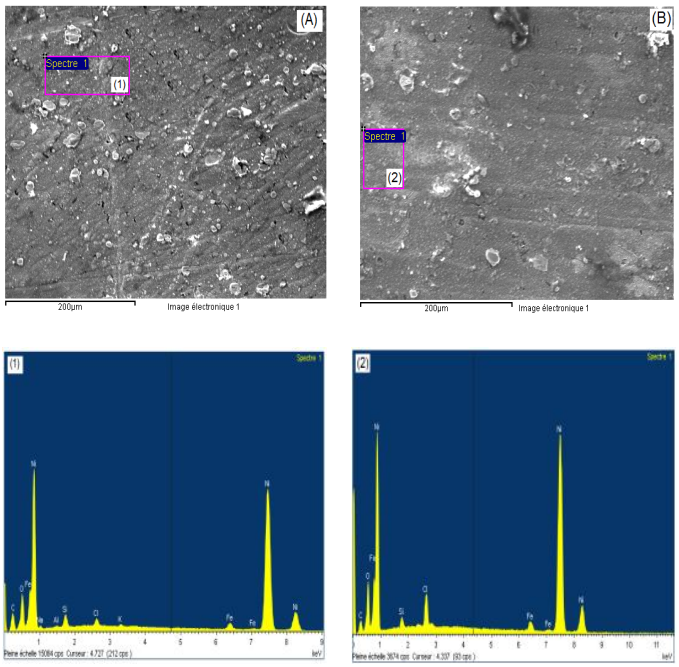

Fig.10. Micrograph (SEM) of (N/SiC) deposition surface on a steel substrate, A) 10 g/l silicon carbide, B) 15 g/l silicon carbide, 1) and 2) associated EDS spectra.

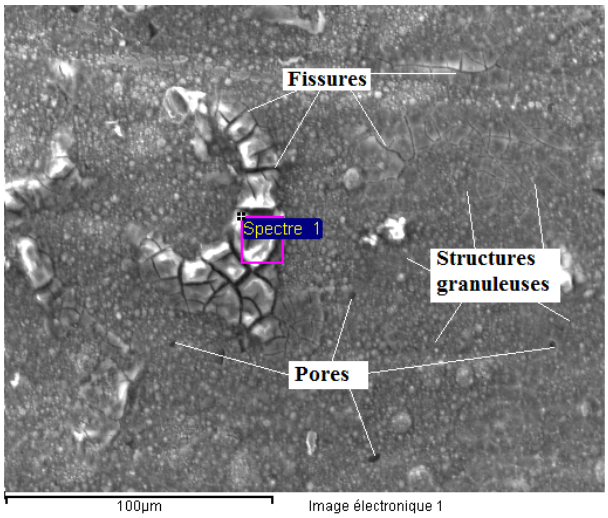

Fig.11. Surface morphology of a composite deposit N/SiC in the presence of 25 g/l of SiC.

The micrograph (SEM) shown in Figure (10.A) shows that Ni-SiC deposition is not homogeneous; we clearly notice empty sites in the form of small crevices giving directly onto the steel substrate. In the presence of aggressive ions, such as chlorides, these crevices can develop into micro-bites creating a galvanic corrosion stack between the steel (anode) and the Ni-SiC composite coating (cathode).

Figure (10.B) shows a more compact and homogeneous deposition as well as in figure (10.A); with a smaller number of crevices.

The EDS analysis of the two spectra, figures (10−1 and 10−2), shows a matrix essentially made of nickel, we note the presence of oxygen and iron revealing the existence of iron oxides formed during electroplating. The chlorine resulting from the deposition bath is also present. Carbon and silicon are also present in small quantities.

According to Fig. 11, with the presence of 25 g/l silicon carbides in the coating bath, it can be seen that the deposit structure is granular, the presence of cracks and pores is also observed, these surface irregularities can facilitate the intrusion of aggressive ions such as chloride ions and therefore, the corrosion rate of the steel substrate is accelerated beyond 15 g/l SiC.

IV. CONCLUSION

- According to the results obtained by weight loss and electrochemical polarization techniques, we notice that the corrosion rate decreases with the increase of Sic concentration up to 15 g/l. this decrease is probably due to the presence of Sic particles leading to improved corrosion resistance. These properties are mainly due to the homogeneous distribution of the constituents (SiC) as determined by the atomic force microscopy technique and the possibilities of combining the characteristics of base metals and their coatings. However, optical observations highlight that for sic concentrations above 20 g/l, the form of corrosion encountered in these cases is pitting corrosion (the number of pits increases with the increase in sic content). The results in local attacks of the passive film due to the presence of the micropiles on the substrate surface may result from the excess of SiC causing heterogeneity in the deposit.
- Atomic force microscopic analysis (AFM) of composite deposits (Ni/SiC) shows a significant evolution of deposit morphology as a function of SiC introduction. Deposits without SiC particles have a very smooth morphology with rare nodules. As the silicon carbide content increases, the deposits become rough and the number of nodules increases randomly with various dimensions. we also observe a microstructural refinement of the deposits as a function of the increase of the silicon carbide content;
- The Ni-SiC composite deposits micrograph (SEM) shows a more compact and homogeneous deposition for concentrations below 15 g/l SiC, and with silicon carbide content above 15 g/l, it can be seen that the deposit structure is granular, the presence of cracks and pores is also canceled, the surface irregularities can be the intrusion of aggressive ions such as chloride ions.

REFERENCES

[1] N. Daemi, F. Mahboubi, H. Alimadadi, Effect of plasma nitriding on electrodeposited Ni–Al composite coating, Mater. Des. 32 (2011) 971–975.

[2] P. Gyftou, E.A. Pavlatou, N. Spyrellis, Effect of pulse electrodeposition parameters on the properties of Ni/nano-SiC composites, Appl. Surf. Sci. 254 (2008) 5910–5916.

[3] A.D. Pogrebnjak, Sh.M. Ruzimov, D.L. Alontseva, P. Zukowski, C. Karwat, C.Kozak, M. Kolasik, Structure and properties of coatings on Ni base deposited using a plasma jet before and after electron a beam irradiation, Vacuum 81(2007) 1243–1251.

[4] I. Garcia, J. Fransaer, J.P. Celis, Surf. Coat. Techol. 148 (2001) 171.

[5] L. Burzynska, E. Rudnik, J. Koza, L. Blaz, S. Wojciech, Surf. Coat. Technol. 202 (2008) 2545.

[6] L. Benea, P.L. Bonora, A. Borello, S. Martelli, F. Wenger, P. Ponthiaux, J. Galland, Solid State Ionics 151 (2002) 89.

[7] Y. Zhou, H. Zhang, B. Qian, Appl. Surf. Sci. 253 (2007) 8335.

[8] S. Xie, X.L. Tong, G.Q. Jin, Y. Qin, X.Y. Guo, CNT-Ni/SiC hierarchical nanostructures: preparation and their application in electrocatalytic oxidation of methanol, J. Mater. Chem. A 1 (2013) 2104–2109.

[9] Y. Wang, H.B. Xu, Preparation and numerical simulation of Ni–SiC composite coatings deposited by electrode position, Res. J. Appl. Sci.,Eng. Technol. 5 (24) (2013) 5602–5607.

[10] Zh. Zengwei, Zh. Di, Q. Ningsong, L.Weining, Electrodeposition of bright nickel coating under perturbation of hard particles, Mater. Des. 28 (2007) 1776–1779.

[11] B. Ranjith, G.P. Kalaignan, Ni–Co–TiO2 nanocomposite coating prepared by pulse and pulse reversal methods using acetate bath, Appl. Surf. Sci. 257 (2010) 42–47.

[12] C.C. Anya, Wet erosive wear of alumina and its composites with SiC nano-particles, Ceram. Int. 24 (1998) 533–542.

[13] Z. Wang, J. Shemilt, P. Xiao, Novel fabrication technique for the production of ceramic/ceramic and metal/ceramic composite coatings, Scr. Mater. 42 (2000) 653–659.

[14] M.J. Jiao, X.X. Wang, Electrolytic deposition of magnesium-substituted hydroxyapatite crystals on titanium substrate, Mater. Lett. 63 (2009) 2286–2290.

[15] E.A. Pavlatou, M. Stroumbouli, P. Gyftou, N. Spyrellis, Hardening effect induced by incorporation of SiC particles in nickel electrodeposits, J. Appl. Electrochem. 36 (2006) 385–394.

[16] Z.H. Zhao, Y. Sakagami, T. Osaka, Chem. Lett. 9 (1997) 909.

[17] M.R. Vaezi, S.K. Sadrnezhaad, L. Nikzad, Colloids Surf. A: Physicochem. Eng.Aspects 315 (2008) 176–182.

[18] T. Lampke, B.Wielage, D. Dietrich, A. Leopold, Appl. Surf. Sci. 253 (2006) 2399–2408.

[19] Q. Zhao, Y. Liu, C. Wang, Appl. Surf. Sci. 252 (2005) 1620.

[20] D.F. Susan, K. Barmak, A.R. Marder, Electrodeposited Ni–Al particle composite coatings, Thin Solid Films 307 (1997) 133–140.

[21] J. Catonné, C. Tournier, Préparation de surfaces Métalliques, Manuel des traitements de surface à l'Usage des Bureaux d'Etudes, Edité par Club des traitements de Surface, Paris, Edition CETIM, (1987).

[22] A. Pollack, Nettoyage et Dégraissage des Métaux, des forges Edition, (1964).

[23] M. Wery, Décapage des Métaux, M1455, Technique de l'Ingénieur, (2000).

[24] R. Tournier, Polissage Mécanique, M1495, Technique de l'Ingénieur, (2000).

[25] J.C. Catonné, Traitements de Surface par Voie Humide : Principe Electrochimique, M1428, Technique de l'Ingénieur, (1990).

[26] J.C Mahieu, B. Oury et A. Boulet, INRS, Caractéristiques de l'émission d'aérosols des bains de nickelage, INRS, 2e trimestre (1990).

[27] P. Benaben, Chromage, M1615, Technique de l'Ingénieur, 2000.

[28] Y. Badé, Revêtements Métalliques par Voie Electrolytique, Cuivrage M1605, Technique de l'Ingénieur, (1990).

[29] Karayianni, H.S., Batis, G., and Vassiliou, P., "Corrosion resistance of composite nickel-Al_2O_3 deposits", Anti-corros. Method M., Vol 46(1), pp. 29-34, (1999).

[30] L. A. Goodman, RCA Rev, 35 (1974) 613.

[31] D. Landot, Corrosion et traitements de surfaces des métaux, Presses Polytechniques et universitaires Romandes, Lausanne, (1993).

[32] Kang, J.X., Zhao, W.Z., Zhang, G.F., "Influence of electrodeposition parameters on the deposition rate and micro hardness of nanocrystalline Ni coatings", Surf. Coat. Technol. Vol 203(13), pp. 1815-1818, (2009).

[33] Chunyang Ma, Guiqiang Liang, Yongyong Zhuc, Haiwei Mu, Fafeng Xia., "Preparation and corrosion assessment of electrodeposited Ni–SiC composite thin films", Ceramics International 40 (2014) ,pp.3341–3346,2013.

[34] K.H. Hou, M.D. Ger, L.M. Wang, S.T. Ke, Wear 253 (2002) 994.

[35] K.C. Chan, C.L. Wang, K.F. Zhang, G. Pang, Scr. Mater. 51 (2004) 605.

[36] Zhongcheng Guo, Xiaoyun Zhu, Mater. Sci. Eng., A Struct. Mater.: Prop. Microstruct. Process. 363 (2003) 325.

[37] B.K. Prasad, Wear 252 (2002) 250.